independent, blind analyses with extracts from over 30 animals. Neither the genetic background of the mice (C57BL/6 or 129/Sv-C57BL/6 hybrid) nor the housing environment (barrier facilities at Vanderbilt University and Washington University) affected the results.
24. T. Ayabe and A. J. Ouellette, unpublished data.
25. Residues 1 to 39 of the cryptdin-1 pro segment (Fig. 2A) were deduced from cDNA sequence (*15*). The peptide was synthesized in solid phase and purified to homogeneity by rpHPLC by Quality Controlled Biochemicals (Hopkinton, MA). The sequence was verified by mass spectrometry and amino acid analysis. After conjugation of the peptide to BSA, polyclonal antiserum to pro segment was produced in a sheep by administration of three to four dorsal subcutaneous injections of BSA-conjugated peptide mixed with an equal volume of complete Freund's adjuvant. Injections were repeated twice, and the antiserum titer was evaluated by enzyme-linked immunosorbent assay by Quality Controlled Biochemicals. The antibody also recognizes proCC, suggesting that it is immunoreactive against multiple procryptdins. The pro segment sequence is highly conserved among the family.
26. R. L. Shattuck-Brandt, L. W. Lamps, K. J. Heppner Goss, R. N. DuBois, L. M. Matrisian, *Mol. Carcinog.* **24**, 177 (1999).
27. D. Darmoul and A. J. Ouellette, *Am. J. Physiol.* **271**, G68 (1996); D. F. Cano-Gauci *et al.*, *Exp. Cell Res.* **208**, 344 (1993).
28. Y. Satoh, Y. Habara, K. Ono, T. Kanno, *Gastroenterology* **108**, 1345 (1995).
29. Crypts were isolated from $MAT^{+/+}$ and $MAT^{-/-}$ males (original 129/Sv-C57BL/6 hybrid backcrossed to C57BL/6 for 10 generations) as described (*27*). Eluted crypts resuspended in ice-cold $Ca^{2+}$- and $Mg^{2+}$-free Hank's balanced salt solution were transferred singly to siliconized microcentrifuge tubes to obtain 1, 5, or 20 crypts per tube; to transfer 100 crypts per tube, we measured crypt numbers with a hemacytometer and transferred appropriate volumes. Crypts were centrifuged at 700*g* for 5 min and resuspended in 30 μl of isotonic PIPES buffer [10 mM PIPES (pH 7.4) and 0.8% NaCl] containing 100 μM CCh to stimulate selectively Paneth cell degranulation (*28*). After a 30-min incubation at 37°C in a rotary shaker at 150 cycles/min, crypts were centrifuged for 5 min at 700*g*, and supernatants containing CCh-induced Paneth cell secretions were harvested aseptically and stored at −20°C.
30. A. J. Ouellette, S. I. Miller, A. H. Henschen, M. E. Selsted, *FEBS Lett.* **304**, 146 (1992).
31. S. J. Hultgren *et al.*, *Cell* **73**, 887 (1993).
32. Male and female $MAT^{+/+}$ and $MAT^{-/-}$ mice (C57BL/6 background) were infected at 5 weeks of age. *Escherichia coli* KBC-236 (in 150 ml of Luria-Bertani broth containing ampicillin and kanamycin) was grown statically for 48 hours at 37°C to induce pili formation. Bacteria were pelleted by centrifugation at 10,000 rpm for 10 min and washed with cold sterile PBS. After recentrifugation, bacteria were resuspended in 1.5 ml of PBS, and the approximate concentration of bacteria was determined by optical density at 600 nm. The actual number of colony-forming units (CFUs) was measured by plating serial dilutions. Mice were made to fast for 2 hours before oral administration of bacteria. Animals were lightly anesthetized with methoxyfluorane and then given a 0.1-ml dose of 0.1 M sodium bicarbonate (to neutralize stomach acids) immediately followed by a 0.1-ml bolus of bacteria (1 to $2 \times 10^{10}$ CFUs) in PBS with a 1-ml syringe fitted with a stainless steel feeding needle. Mice were given access to food 30 min after inoculation. After 2 hours, mice were anesthetized and killed by cervical dislocation. The small intestine was removed en bloc and cut into three portions of equal length (proximal, mid, and distal segments). Each segment was homogenized in 3 ml of PBS and serially diluted for plating on kanamycin for determination of CFUs per milliliter.
33. S. C. Gad and C. S. Weil, in *Principles and Methods of Toxicology*, A. W. Hayes, Ed. (Raven, New York, 1989), pp. 463–467; S. Welkos and A. O'Brien, *Methods Enzymol.* **235**, 29 (1994).
34. A. J. H. Gearing *et al.*, *Nature* **370**, 555 (1994); P. A. Marcotte, I. M. Kozan, S. A. Dorwin, J. M. Ryan, *J. Biol. Chem.* **267**, 13803 (1992).
35. Paneth cell secretory granules were prepared from enriched crypt fractions from duodenum and ileum. Crypts dissociated from the lamina propria with EDTA (*27*) were resuspended in ice-cold $Ca^{2+}$- and $Mg^{2+}$-free Hank's balanced salt solution, and cells were lysed in a Parr cavitation bomb. After an initial centrifugation of cell lysate at 700*g*, granules were pelleted from the supernatant at 27,000*g* for 40 min.
36. We thank R. P. Mecham, T. J. Broekelmann, and A. H. Henschen for protein sequencing; M. E. Selsted for the antibody to cryptdin-1, the cryptdin-4 peptide standard, and helpful discussions; M. A. Mulvey for help with bacteria and critical review of the manuscript; F. Heffron for the virulent *S. typhimurium* strain 14028s; and S. Shapiro and J. Lohi for insightful comments on the manuscript. All animal experiments were performed with the approval of the Washington University School of Medicine Animal Studies Committee. This work was supported by a Barnes-Jewish Hospital Foundation grant (to C.L.W.) and by grants from NIH (to W.C.P., A.J.O., L.M.M., and S.J.H.).

7 May 1999; accepted 20 August 1999

# Est1 and Cdc13 as Comediators of Telomerase Access

**Sara K. Evans and Victoria Lundblad***

Cdc13 and Est1 are single-strand telomeric DNA binding proteins that contribute to telomere replication in the yeast *Saccharomyces cerevisiae*. Here it is shown that fusion of Cdc13 to the telomerase-associated Est1 protein results in greatly elongated telomeres. Fusion proteins consisting of mutant versions of Cdc13 or Est1 confer similar telomere elongation, indicating that close physical proximity can bypass telomerase-defective mutations in either protein. Fusing Cdc13 directly to the catalytic core of telomerase allows stable telomere maintenance in the absence of Est1, consistent with a role for Est1 in mediating telomerase access. Telomere length homeostasis therefore is maintained in part by restricting access of telomerase to chromosome termini, but this limiting situation can be overcome by directly tethering telomerase to the telomere.

In most species, telomeres are composed of G-rich repetitive sequences that are elongated by telomerase (*1*). Several factors govern the balance between sequence addition and loss to maintain telomeres at a stable length, including positive and negative regulation of telomerase access to the chromosome terminus (*2–4*). In *S. cerevisiae*, five genes are required for the telomerase pathway (*4–7*). *TLC1* and *EST2* encode the RNA and reverse transcriptase subunits of telomerase, respectively, and as expected for subunits that are essential for catalysis, telomerase activity is absent in extracts from strains defective in *EST2* or *TLC1*(*7–9*). In contrast, mutations in *EST1*, *EST3*, and *CDC13* do not eliminate enzyme activity in vitro (*9*, *10*), despite the fact that strains carrying mutations in any of these three genes have the same severe telomere replication defect as *est2*-Δ or *tlc1*-Δ strains (*6*, *10*).

Both Cdc13 and Est1 bind single-strand telomeric DNA (*4*, *11*, *12*), although they make separate contributions to telomere replication and stability. Est1 is required solely for the telomerase pathway (*11*), whereas Cdc13 has an essential function at the telomere, presumably in protecting the end of the chromosome (*13*), as well as a role in telomere replication (*4*). This latter activity was revealed by a telomerase-defective allele of Cdc13, called $cdc13^{est}$ [originally named *est4* (*6*)], leading to the proposal that Cdc13, like Est1, mediates telomerase access (*4*). The two proteins also display different biochemical properties. Est1, but not Cdc13, requires a free single-strand 3′ terminus for DNA binding and binds telomeric DNA with a 500-fold reduced affinity compared with Cdc13 (*4*, *11*). In addition, Est1 is associated with telomerase, whereas Cdc13 does not exhibit a detectable interaction with the enzyme (*14*).

These results suggest that telomerase is recruited to the telomere due to a direct (but weak) protein-protein interaction between Cdc13 and the enzyme, and the telomere shortening in the $cdc13^{est}$ mutant strain is due to a further reduction in this interaction. This model predicts that increasing the association between Cdc13 and telomerase would increase telomere length. To test this, we examined the consequences of fusing Cdc13 to the telomerase-associated protein Est1 (*15*). Introduction of the gene encoding this Cdc13-Est1 fusion, present on a single-copy plasmid and expressed by the *CDC13* promoter, into a $CDC13^{+}$ strain resulted in substantial telomere elongation (Fig. 1A, lanes 2

Department of Molecular and Human Genetics, and Verna and Marrs McLean Department of Biochemistry, Baylor College of Medicine, Houston, TX 77030, USA.

*To whom correspondence should be addressed: E-mail: lundblad@bcm.tmc.edu

and 3). This effect was dependent on functional telomerase, because telomeres were not elongated when the fusion was introduced into an *est2*-Δ strain (Fig. 1A, lanes 14 to 16). Telomere elongation was even more pronounced in a *cdc13*-Δ strain, in which telomere length increased by ~800 base pairs after ~100 generations of growth (Fig. 1A, lanes 4 and 5); continued propagation resulted in even further telomere lengthening (*16*).

Several experiments indicated that both Cdc13 and Est1 retained function in the context of the fusion. First, the essential function of *CDC13* was fully complemented by the fusion protein (Fig. 1B). The Cdc13-Est1 fusion also complemented the senescence phenotype of an *est1*-Δ strain (Fig. 1C). This was not due to a general bypass of the telomerase pathway, because this same fusion did not complement *est2*-Δ or *est3*-Δ strains (Fig. 1C). The complementation behavior of the fusion protein indicates that Est1 and Cdc13 normally function in temporal and physical proximity in their respective roles in telomere replication. Telomerase also has been shown to coimmunoprecipitate with Est1 but not with Cdc13 (Fig. 1D) (*14*). The Cdc13-Est1 fusion protein coimmunoprecipitated the RNA subunit of the telomerase complex (Fig. 1D) and enzyme activity (*17*), indicating that telomerase is associated with the fusion protein.

These results suggest that the proposed recruitment function of Cdc13 can be enhanced by fusing it to a telomerase component, and predict that the telomerase-defective *cdc13$^{est}$* mutation would be bypassed in a fusion. Consistent with this prediction, a fusion containing the mutant Cdc13$^{est}$ protein behaved indistinguishably from the wild-type (WT) fusion: Telomere elongation occurred to the same degree in both *CDC13*$^+$ and *cdc13*-Δ strains (Fig. 1A, compare lanes 6 to 9 and 2 to 5), and no senescence was observed when the Cdc13$^{est}$-Est1 fusion was introduced into a *cdc13*-Δ strain (*17*). Similar results were observed in a reciprocal experiment with a mutant allele of *EST1* (*est1-47*); this mutation disrupts telomere replication

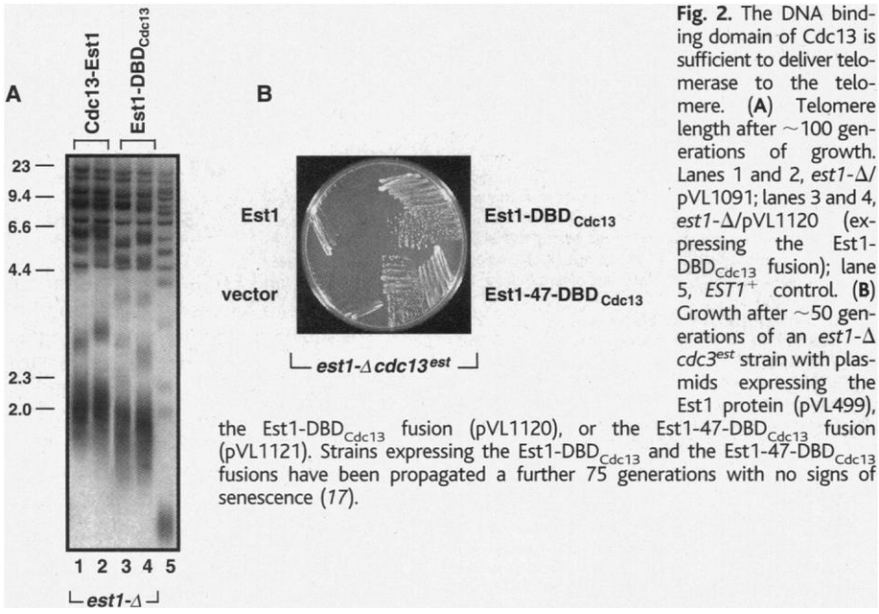


**Fig. 2.** The DNA binding domain of Cdc13 is sufficient to deliver telomerase to the telomere. (**A**) Telomere length after ~100 generations of growth. Lanes 1 and 2, *est1*-Δ/pVL1091; lanes 3 and 4, *est1*-Δ/pVL1120 (expressing the Est1-DBD$_{Cdc13}$ fusion); lane 5, *EST1*$^+$ control. (**B**) Growth after ~50 generations of an *est1*-Δ *cdc3$^{est}$* strain with plasmids expressing the Est1 protein (pVL499), the Est1-DBD$_{Cdc13}$ fusion (pVL1120), or the Est1-47-DBD$_{Cdc13}$ fusion (pVL1121). Strains expressing the Est1-DBD$_{Cdc13}$ and the Est1-47-DBD$_{Cdc13}$ fusions have been propagated a further 75 generations with no signs of senescence (*17*).

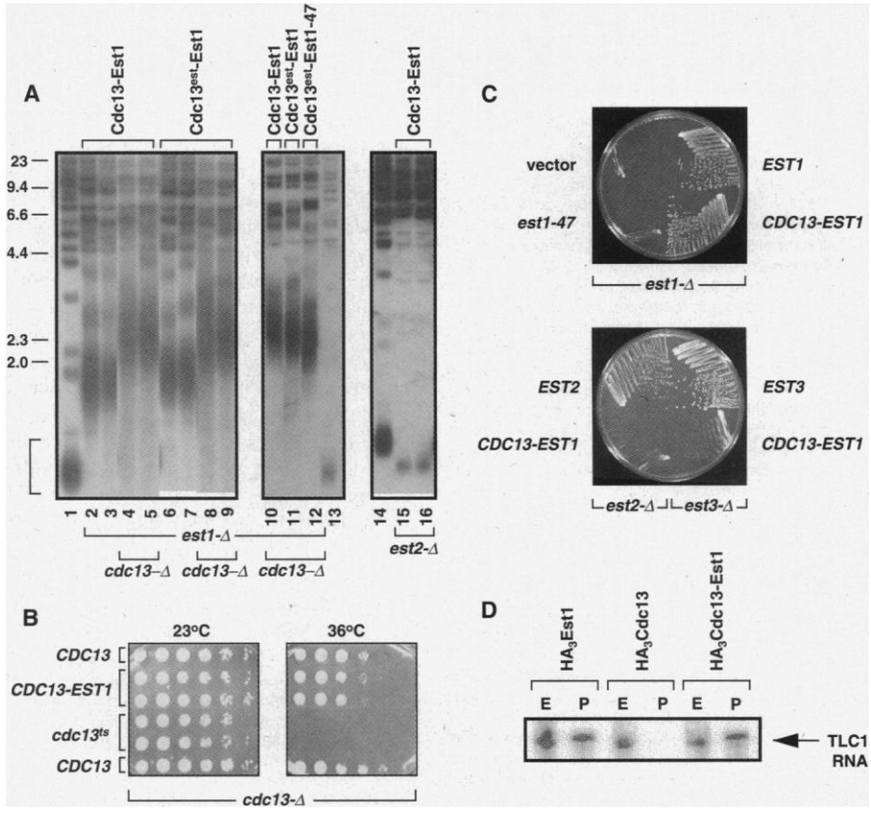


**Fig. 1.** The Cdc13-Est1 fusion confers telomere elongation. (**A**) Telomere Southern (DNA) blots were performed as in (*6*). The bracket indicates a heterogeneous telomeric band that represents about two-thirds of the telomeres in this strain background. Cultures for lanes 1 to 13 were grown for ~100 generations before DNA preparation. Lanes 1, 13, and 14, *CDC13*$^+$ *EST*$^+$ control strain; lanes 2 to 5, 10, 15, and 16, pVL1091 (expressing the Cdc13-Est1 fusion); lanes 6 to 9 and 11, pVL1092 (Cdc13$^{est}$-Est1); lane 12, pVL1098 (Cdc13$^{est}$-Est1-47); the relevant genotypes of the strains are indicated. Plasmids were introduced into strains deleted for *CDC13* for this and subsequent figures by first transforming into a *cdc13*-Δ/pVL438 (*CDC13*$^+$ *URA3*$^+$) strain followed by subsequent eviction of pVL438 by plating on media containing 5-fluoro-orotic acid. Molecular sizes are indicated on the left (in kilobase pairs). (**B**) *cdc13*-Δ strains containing pVL648 (*CDC13*$^+$), pVL1091, or pVL762 (*cdc13$^{ts}$*) (*13*) were grown at 23°C, and equivalent numbers of cells, as serial 10-fold dilutions, were plated at 23° and 36°C. (**C**) Growth after ~50 generations of *est1*-Δ, *est2*−Δ , or *est3*-Δ strains, with single-copy plasmids bearing the *CDC13-EST1* fusion gene or the appropriate WT *EST* gene (each under their native promoter). (**D**) Immunoprecipitation from extracts prepared from strains expressing proteins with a triple hemagglutinin epitope (HA$_3$) introduced at the NH$_2$-terminus: HA$_3$Est1 (pVL1106), HA$_3$Cdc13 (pVL841), or HA$_3$Cdc13-Est1 (pVL1102), followed by detection of the telomerase RNA (TLC1) levels in the extract (E) and immunoprecipitates (P) by Northern (RNA) blotting (*27*).

(Fig. 1C), although the mutant Est1 protein still physically associates with telomerase (*18*), suggesting a defect in the same telomerase-accessing function that is altered by the *cdc13*$^{est}$ allele. This defect was bypassed when the Est1-47 protein was fused to Cdc13. In fact, the double-mutant fusion protein (Cdc13$^{est}$ fused to Est1-47) conferred the same degree of telomere elongation as the WT fusion protein, even in a strain deleted for both *est1*-Δ and *cdc13*-Δ (Fig. 1A, lane 12); moreover, this strain did not exhibit senescence (*17*). The ability of the double-mutant fusion to complement a *cdc13*-Δ *est1*-Δ strain indicates that the fusion is acting as a dimeric molecule that bridges telomerase and the telomere.

One alternative interpretation of our data is that telomere elongation is due to perturbation of chromatin structure, rather than to increased access of telomerase to the telomere. In particular, telomere lengthening could be a secondary consequence of altered Cdc13 function, because mutations in *CDC13* have been identified that increase telomere length (*19*, *20*). However, these recessive alleles of *CDC13* have a set of genetic and biochemical features that distinguish them from the gain-of-function properties of the Cdc13-Est1 fusion (*17*, *20*). In addition, fusion of several unrelated protein sequences, or an inactive telomerase subunit (see below), to the COOH-terminus of either the WT Cdc13 protein or the mutant Cdc13$^{est}$ protein does not increase telomere length (*17*, *21*). The most direct argument against this alternative interpretation is the result of an experiment in which we examined the behavior of a fusion in which only the high-affinity DNA binding domain of Cdc13 ($DBD_{Cdc13}$) was fused to Est1 (*15*). This experiment was based on our previous demonstration that $DBD_{Cdc13}$ can be expressed as a stable, functional subdomain (*22*) and therefore could be used as an alternative means of directing Est1 to the telomere with high efficiency, while leaving the full-length Cdc13 protein intact. As predicted, the Est1-$DBD_{Cdc13}$ fusion conferred extensive telomere lengthening in a *CDC13*$^{+}$ strain (Fig. 2A) and bypassed senescence of a *cdc13*$^{est}$ strain (Fig. 2B). Furthermore, fusion of the defective Est1-47 protein to $DBD_{Cdc13}$ bypassed both *est1*-Δ and *cdc13*$^{est}$ mutations (Fig. 2B), even though the *est1-47* allele fails to complement either mutation (Fig. 1C) (*17*). Expression of either Est1 or $DBD_{Cdc13}$ had no effect on telomere length or viability in *CDC13*$^{+}$ or *cdc13*$^{est}$ strains, and the Est1-$DBD_{Cdc13}$ fusion failed to rescue the inviability of a *cdc13*-Δ strain (Fig. 2A) (*17*). Thus, the telomere lengthening properties of these fusions are likely to be a consequence of delivery of telomerase to the telomere, rather than a perturbation of Cdc13 function.

We next fused Cdc13 directly to Est2, the catalytic subunit of telomerase (*8*). The Cdc13-Est2 fusion (*15*) resulted in telomere lengthening to levels comparable to that of the Cdc13-Est1 fusion (Fig. 3A, lanes 3 and 4). The fusion complemented *cdc13*-Δ and *est2*-Δ null mutations, and telomere elongation occurred to the same degree in *est2*-Δ and *EST2*$^{+}$ strains (*17*). A Cdc13-$Est2_{D670A}$ fusion, containing an Asp to Ala mutation at position 670 in the active site of Est2 (*8*), did not confer extensive telomere elongation but instead maintained telomere length at WT levels in a *cdc13*-Δ *EST2*$^{+}$ strain (Fig. 3A, lanes 5 and 6) (*23*), showing that telomere elongation is only observed when a catalytically active version of telomerase is tethered to the telomere. Strikingly, the Cdc13-Est2 fusion allowed cell growth in the complete absence of Est1 function, because an *est1*-Δ strain carrying this fusion was viable for more than 250 generations (Fig. 3B) (*24*). Long-term propagation in the absence of Est1 was not due to a previously described alternative pathway that can maintain telomeres in the absence of telomerase function (*6*, *25*): Telomeres in an *est1*-Δ strain carrying the Cdc13-Est2 fusion were stably maintained at a length slightly below that of WT telomere length (Fig. 3C), with none of the striking changes in telomere structure that characterize the alternative pathway (*6*, *25*). The ability of the Cdc13-Est2 fusion to maintain an *est1*-Δ strain required tethering of a functional telomerase, because an *est1*-Δ strain carrying the Cdc13-$Est2_{D670A}$ fusion exhibited senescence (Fig. 3B). This supports the hypothesis that a critical function of the Est1 protein is to mediate access of telomerase to the telomere. Notably, neither the Cdc13-Est1 fusion nor the Cdc13-Est2 fusion bypassed the requirement for Est3 (Fig. 1C) (*17*), showing that Est1 and Est3 perform functionally distinct roles in telomere replication.

Our results are consistent with a model in which Cdc13 mediates telomerase access by a direct interaction with the enzyme (Fig. 4). Furthermore, these data indicate that Est1 is a comediator of this "accessing" function, potentially as a direct binding partner of Cdc13, although we cannot rule out the possibility of

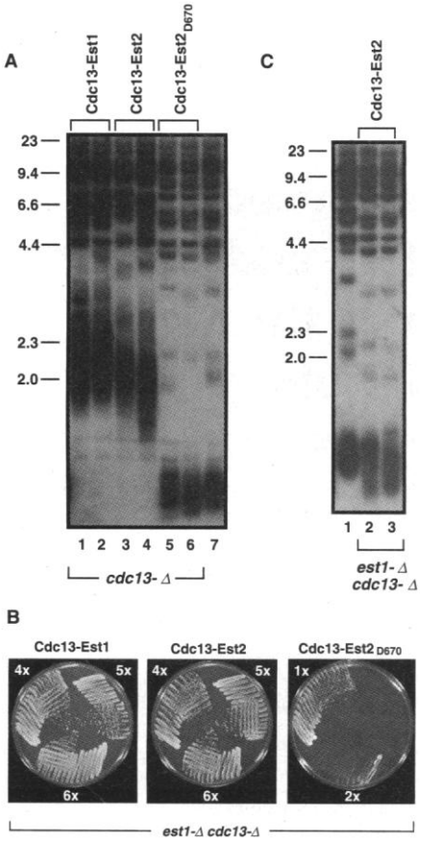


**Fig. 3.** Fusing Cdc13 to the catalytic subunit of telomerase bypasses the requirement for Est1. **(A)** Telomere length, after ~75 generations of growth. Lanes 1 and 2, *cdc13*-Δ/pVL1091; lanes 3 and 4, *cdc13*-Δ/pVL1107 (expressing the Cdc13-Est2 fusion); lanes 5 and 6, *cdc13*-Δ/pVL1111 (Cdc13-$Est2_{D670}$); lane 7, *CDC13*$^{+}$ control strain. **(B)** Growth of an *est1*−Δ *cdc13*-Δ strain with either pVL1091 or pVL1107 for ~100 (4×) to ~150 (6×) generations after eviction of the *CDC13* plasmid. The *est1*-Δ *cdc13*-Δ/pVL1111 (Cdc13-$Est2_{D670}$) strain (constructed by dissection of a *est1*-Δ/*EST1*$^{+}$ *cdc13*-Δ/*CDC13*$^{+}$ diploid strain with pVL1111) is shown after ~25 and ~50 generations of growth. **(C)** Telomere length, after ~150 generations of growth, of a *CDC13*$^{+}$ *EST*$^{+}$ control strain (lane 1) or an *est1*−Δ *cdc13*-Δ/pVL1107 strain (lanes 2 and 3). This strain has been propagated for an additional ~125 generations with no signs of senescence or changes in telomere length (*17*).

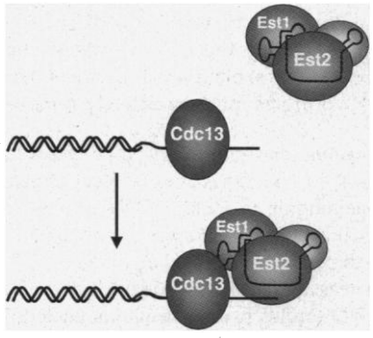


**Fig. 4.** Model for Cdc13 and Est1 as positive regulators of telomerase function. Cdc13 is proposed to bind the single-stranded overhang present at the ends of chromosomes and to mediate telomerase access by a direct but weak protein interaction with a component of the telomerase holoenzyme, possibly Est1. Telomerase is shown as a multisubunit RNA-containing complex that may include additional proteins such as Est3 (*14*). In addition to the positive regulation described here, telomeres are also subject to negative length regulation in both yeast and human cells, which has been proposed to be mediated by cis-inhibition of telomerase through the action of duplex telomere DNA binding proteins (*3*). Whether Est1 and Cdc13 are the direct recipients of such negative regulators is an intriguing question.

additional intervening protein or proteins. These experiments may have also uncovered an additional role for Est1 in telomerase function, as the Cdc13-Est2 fusion was not capable of promoting extensive telomere elongation in the absence of Est1 (Fig. 3C) (*26*). Because Est1 is a terminus-specific DNA binding protein (*11*), we speculate that this second role may be to promote accessibility of the 3′ terminus to the active site of telomerase.

### References and Notes


1. C. I. Nugent and V. Lundblad, *Genes Dev.* **12**, 1073 (1998).
2. J. Shampay and E. H. Blackburn, *Proc. Natl. Acad. Sci. U.S.A.* **85**, 534 (1988).
3. S. Marcand, E. Gilson, D. Shore, *Science* **275**, 986 (1997); B. van Steensel and T. de Lange, *Nature* **385**, 740 (1997); S. Marcand, V. Brevet, E. Gilson, *EMBO J.* **18**, 3509 (1999).
4. C. I. Nugent, T. R. Hughes, N. F. Lue, V. Lundblad, *Science* **274**, 249 (1996).
5. V. Lundblad and J. W. Szostak, *Cell* **57**, 633 (1989).
6. T. S. Lendvay, D. K. Morris, J. Sah, B. Balasubramanian, V. Lundblad, *Genetics* **144**, 1399 (1996).
7. M. S. Singer and D. E. Gottschling, *Science* **266**, 404 (1994).
8. J. Lingner *et al.*, *ibid.* **276**, 561 (1997).
9. M. Cohn and E. H. Blackburn, *ibid.* **269**, 396 (1995).
10. J. Lingner, T. R. Cech, T. R. Hughes, V. Lundblad, *Proc. Natl. Acad. Sci. U.S.A.* **94**, 11190 (1997).
11. V. Virta-Pearlman, D. K. Morris, V. Lundblad, *Genes Dev.* **10**, 3094 (1996).
12. J. J. Lin and V. A. Zakian, *Proc. Natl. Acad. Sci. U.S.A.* **93**, 13760 (1996).
13. B. Garvik, M. Carson, L. Hartwell, *Mol. Cell. Biol.* **15**, 6128 (1995).
14. T. R. Hughes, S. K. Evans, R. G. Weilbaecher, V. Lundblad, in preparation.
15. In-frame fusion proteins were constructed as follows: The Cdc13-Est1 fusion (pVL1091) fused $Cdc13_{1-924}$-$Est1_{6-699}$; the Cdc13-Est2 (pVL1107) and Cdc13-$Est2_{D670A}$ (pVL1111) proteins fused $Cdc13_{1-924}$-$Est2_{1-884}$. All three constructs were expressed from the genomic *CDC13* promoter and derived from the single-copy *CEN* plasmid, pRS415. The Est1-$DBD_{Cdc13}$ and Est1-47-$DBD_{Cdc13}$ fusions (pVL1120 and pVL1121, respectively), expressed in single copy from the *EST1* promoter, fused the Cdc13 DNA binding domain (*22*) to the COOH terminus of Est1, to generate $Est1_{1-699}$ - $Cdc13_{2-21,452-693}$. Telomere elongation by any of these fusion proteins is not due to increased protein expression in the context of the fusion, because overexpression of Est1, Est2, or Cdc13, or expression of Est1 by the *CDC13* promoter, has little or no effect on telomere length (*8*, *11*, *17*, *19*).
16. We have also observed up to a ~4-kb increase in the length of a single telomere (chromosome IIIL). Strains with greatly elongated telomeres do not exhibit any discernable growth defect but were not examined for more subtle defects (such as alterations in cell cycle progression). We have not investigated yet whether the increase in telomere length in strains carrying Cdc13-telomerase fusions occurs at a constant rate, or if there is some influence of cis-inhibition on elongation, as previously observed (*3*).
17. S. K. Evans and V. Lundblad, unpublished data.
18. The *est1-47* mutation is one of a panel of alanine-scan mutations in *EST1* (*17*); the Est1-47 mutant protein still retains association with telomerase (at 20% of WT levels), as assessed by coimmunoprecipitation with the TLC1 RNA (*27*).
19. N. Grandin, S. I. Reed, M. Charbonneau, *Genes Dev.* **11**, 512 (1997).
20. A. Chandra, T. R. Hughes, V. Lundblad, unpublished data.
21. C. I. Nugent, E. Pennock, V. Lundblad, unpublished data.
22. T. R. Hughes, R. G. Weilbaecher, V. Lundblad, in preparation.
23. Previous work showed that high-level expression of the $Est2_{D670A}$ mutant protein (under the control of the *ADH* promoter, on a 2μ high-copy plasmid) resulted in substantially shorter telomeres in an *EST2*$^+$ strain (*8*). The lack of an effect of the Cdc13-$Est2_{D670A}$ fusion on WT telomere length (Fig. 3A) is presumably a consequence of the lower levels of this fusion protein (confirmed by protein immunoblotting analysis), due to single-copy plasmid expression by the *CDC13* promoter. As expected, the Cdc13-$Est2_{D670A}$ fusion failed to complement an *est2*-Δ strain.
24. Bypass of *est1*-Δ senescence was not simply a consequence of increased Est2 levels (due to possible minimal increase in expression of *EST2* by the *CDC13* promoter), because even higher level expression of *EST2* by the constitutive *ADH* promoter (*8*) was not sufficient to allow an *est1*-Δ strain to grow (*17*).
25. V. Lundblad and E. H. Blackburn, *Cell* **73**, 347 (1993).
26. Association of Cdc13-Est2 fusion protein with the TLC1 RNA was reduced by less than twofold in the absence of Est1, as assessed by immunoprecipitation (*27*), arguing that the failure to elongate telomeres in an *est1*-Δ strain is not simply due to reduced stability of the Cdc13-Est2 telomerase complex.
27. For each sample, cells were grown in selective media to an optical density (600 nm) of 1.0. Cells were harvested by centrifugation and the cell pellets were washed in water and then in TMG 300+ [10 mM tris-HCl (pH 8.0), 1 mM $MgCl_2$, 5% glycerol, 1 mM phenylmethylsulfonyl fluoride, 300 mM NaCl]. Cell extracts were prepared by five repeated cycles of freezing and grinding in liquid nitrogen. Extracts were cleared twice by centrifugation for 10 min at 14,000 rpm at 4°C and immunoprecipitated with an antibody to hemagglutinin (HA) (16β12, Babco) and protein A/G agarose beads (Calbiochem). RNA was prepared by SDS–phenol-chloroform extraction, and TLC1 was detected on 7 M urea–4% polyacrylamide gel as described (*8*). The efficiency of TLC1 recovery in immunoprecipitates is typically less than 2%; the recovery with untagged proteins was less than 0.05%.


28. We thank T. Hughes, R. Weilbaecher, and L. Zumstein for critical review of the manuscript. Supported by NIH grant RO1GM55867 (V.L.) and by a U.S. Army Breast Cancer Research Predoctoral Traineeship (S.K.E.).

9 June 1999; accepted 30 August 1999


# Protamine-Induced Condensation and Decondensation of the Same DNA Molecule


**Laurence R. Brewer,[1] Michele Corzett,[2] Rod Balhorn[2]**



**The DNA in sperm and certain viruses is condensed by arginine-rich proteins into toroidal subunits, a form of packaging that inactivates their entire genome. Individual DNA molecules were manipulated with an optical trap to examine the kinetics of torus formation induced by the binding of protamine and a subset of its DNA binding domain, $Arg_6$. Condensation and decondensation experiments with λ-phage DNA show that toroid formation and stability are influenced by the number of arginine-rich anchoring domains in protamine. The results explain why protamines contain so much arginine and suggest that these proteins must be actively removed from sperm chromatin after fertilization.**


Protamine and other polycations have been shown to coil DNA into toroidal structures containing up to 60 kb of DNA (*1*–*3*). Individual bacteriophage appear to contain a single toroid folded inside the protein capsid (*3*), whereas a sperm cell contains as many as 50,000 toroids packed inside its nucleus (*1*). The protamines responsible for inducing torus formation and packaging DNA in maturing spermatids contain a series of arginine-rich anchoring domains (*4*) that bind to the phosphodiester backbone of DNA in a base sequence–independent fashion (*5*). One protamine molecule is bound to each turn [~11 base pairs (bp)] of DNA (*5*, *6*), and adjacent arginines in the anchoring domains interlock both strands of the helix. Arginine-rich sequences are also present in the proteins that package DNA in several viruses (*7*), but the viral proteins contain fewer anchoring domains per molecule.

In vitro studies using light scattering (*8*, *9*), electron and atomic force microscopy (*1*, *2*, *10*), fluorescence microscopy (*11*, *12*), and DNA elasticity measurements (*13*) have examined how protamine and other polycations induce torus formation. The interpretation of light-scattering experiments has been complicated by DNA aggregation, whereas electron and atomic force microscopy studies characterized only the structure of the final product. Toroid formation and the kinetics of the condensation process could not be observed by fluorescence microscopy because the molecules were not sufficiently extended. To examine toroid formation under conditions that preclude aggregation and precipitation and allow a detailed analysis of kinetics, we used an optical trap to isolate individual DNA molecules and fluorescence microscopy to monitor the formation of toroids in real time


[1]Electronics Engineering Technologies Division, [2]Biology and Biotechnology Research Program, Lawrence Livermore National Laboratory, Livermore, CA 94550, USA.